Journal for ImmunoTherapy of Cancer

Cell-intrinsic PD-L1 signaling drives immunosuppression by myeloid-derived suppressor cells through IL-6/Jak/Stat3 in PD-L1-high lung cancer

Hyein Jeong,[1,2] Jaemoon Koh,[3] Sehui Kim,[4] Jeemin Yim,[3,5] Seung Geun Song,[3,6,7] Hanbyeol Kim,[1,6,7,8] Yingying Li,[1,6,7,8] Soo Hyun Lee,[1,6,7,8] Yeon Kyu Chung,[9] Hongsoon Kim,[1,2] Chul-Hwan Lee,[1,6,7,8] Hye Young Kim,[6,7,10] Bhumsuk Keam ,[1,11] Se-Hoon Lee,[12,13] Doo Hyun Chung,[3,6,7] Yoon Kyung Jeon [1,2,3,14]

To cite: Jeong H, Koh J, Kim S, *et al*. Cell-intrinsic PD-L1 signaling drives immunosuppression by myeloid-derived suppressor cells through IL-6/Jak/Stat3 in PD-L1-high lung cancer. *Journal for ImmunoTherapy of Cancer* 2025;**13**:e010612. doi:10.1136/jitc-2024-010612

► Additional supplemental material is published online only. To view, please visit the journal online (https://doi.org/10.1136/jitc-2024-010612).

Accepted 24 February 2025

For numbered affiliations see end of article.

Correspondence to
Dr Yoon Kyung Jeon;
ykjeon@snu.ac.kr

ABSTRACT

Background Some patients with non-small-cell lung cancer (NSCLC) benefit from immune checkpoint inhibitors (ICIs) despite programmed death-ligand 1 (PD-L1) expression. To address the mechanism of ICI resistance in PD-L1-positive NSCLC, we investigated the role of tumor-cell-intrinsic function of PD-L1 in interleukin (IL)-6-mediated immunosuppression.

Methods Cohorts of NSCLC patients treated with ICI and public datasets were analyzed. PD-L1-overexpressing and PD-L1-knockdown NSCLC cells were submitted to RNA-seq, in vitro analyses, chromatin immunoprecipitation-qPCR, CUT&Tag, and biochemical assays. Human myeloid-derived suppressor cells (MDSCs) sorted from peripheral blood mononuclear cells were co-cultured with NSCLC cells and then assessed for their immunosuppressive activity on T-cells. Mouse Lewis lung carcinoma (LLC) cells with PD-L1 overexpression or knockdown were subcutaneously injected into wild-type or PD-1-knockout C57BL/6 mice in the presence of IL-6 and/or PD-1 blockade.

Results In the ICI cohort with RNA-seq data, the IL-6/Jak/Stat3 pathway was enriched, and IL-6 expression was higher in patients with PD-L1-high NSCLCs who did not respond to ICIs. In another cohort, a higher baseline serum IL-6 level was associated with poor clinical outcomes after ICI therapy. IL-6 expression and the IL-6/Jak/Stat3 pathway were enhanced in PD-L1-high NSCLCs in the ICI cohorts and The Cancer Genome Atlas analysis. IL-6 expression correlated positively with tumor-infiltrating MDSCs in NSCLCs. In NSCLC cells, PD-L1 activated Jak2/Stat3 signaling by binding to and inhibiting protein tyrosine phosphatase 1B. PD-L1 also bound to p-Stat3 in the nucleus, thus promoting the activity of p-Stat3 in the transcription of several cytokines (IL-6, TGF-β, TNF-α, IL-1β) and chemokines. PD-L1-overexpressing NSCLC cells enhanced the migration and immunosuppressive activity of human MDSCs in vitro, mediated by IL-6 and CXCL1. In both wild-type and PD-1-knockout mice, PD-L1-overexpressing LLC tumors were infiltrated by increased MDSCs with high immunosuppressive function, increased Tregs, and decreased granzyme B^+ or $IFN\gamma^+$ CD8 T-cells. These responses were mediated by IL-6 secreted from PD-L1-overexpressing tumor cells. Combined blockade of PD-1 and IL-6 was effective in tumor control and decreased MDSCs while increasing granzyme B^+ or $IFN\gamma^+$ CD8 T-cells.

Conclusions The tumor-cell-intrinsic function of PD-L1 drives immunosuppression and tumor progression through the PD-L1/Jak/Stat3/IL-6/MDSC axis. This pathway represents a potential therapeutic target to improve ICI efficacy in PD-L1-high NSCLC.

WHAT IS ALREADY KNOWN ON THIS TOPIC

⇒ In addition to the conventional role of programmed cell death-ligand 1 (PD-L1) as a ligand for the programmed cell death 1 (PD-1) receptor in the immune checkpoint pathway, its intrinsic function has been increasingly recognized. We investigated the mechanisms by which tumor-cell-intrinsic PD-L1 suppresses antitumor immunity and drives resistance to immune checkpoint inhibitors (ICIs) in non-small-cell lung cancer (NSCLC).

WHAT THIS STUDY ADDS

⇒ This study demonstrates that tumor-cell-intrinsic PD-L1 activates Jak2/Stat3 signaling by inhibiting protein tyrosine phosphatase 1B and binding to phosphorylated Stat3 in the nucleus, enhancing its IL-6 and CXCL1 transcriptional activity. These factors drive immunosuppression via myeloid-derived suppressor cells (MDSCs) and resistance to ICIs in PD-L1-high NSCLC. In a preclinical model of lung cancer, combined therapy targeting IL-6 and PD-1 effectively controlled tumors by reversing MDSC-mediated immunosuppression.

HOW THIS STUDY MIGHT AFFECT RESEARCH, PRACTICE OR POLICY

⇒ The cell-intrinsic PD-L1/Jak2/Stat3/IL-6/MDSC axis represents both a potential biomarker for ICI therapy and a target. Strategies to improve the ICI efficacy in patients with PD-L1-high NSCLC could include antibodies or agents that inhibit, degrade, or relocate PD-L1.

BACKGROUND

Immunotherapy targeting the programmed cell death 1 (PD-1)/programmed death-ligand 1 (PD-L1) pathway can prolong the survival of patients with non-small-cell lung cancer (NSCLC), particularly those with PD-L1-positive NSCLC. However, only approximately 40% of patients with PD-L1-positive NSCLC benefit from immune checkpoint inhibitor (ICI) therapy.[1 2] Thus, to discover novel predictive biomarkers for ICI and to develop effective combined therapies, understanding the mechanism of ICI resistance in PD-L1-positive NSCLC is crucial.

The engagement of PD-L1 with its receptor, PD-1, expressed on the surface of T-cells suppresses T-cell functions.[3] In addition to its role as a ligand for the PD-1 receptor, the intrinsic function of PD-L1 drives several cellular processes,[4 5] including the promotion of cell proliferation, epithelial-mesenchymal transition, and angiogenesis, as well as the regulation of glucose metabolism, the DNA damage response, and immune responses.[4 6–15] Thus, PD-L1 is a multifaceted molecule that is important in cancer progression and resistance to therapy, via its cell-extrinsic and cell-intrinsic signals and its immune-dependent and immune-independent activities.

PD-L1 signaling can occur from the cell surface, cytoplasmic, and nucleus.[4 5] The intracellular localization of PD-L1 is regulated by its post-translational modification and its interaction with cytoskeletal or signaling molecules.[7 8 16] During cytoplasmic and nuclear signaling, PD-L1 interacts with diverse proteins and nucleic acids.[7 12 14 16] Nuclear PD-L1 bound to DNA upregulates genes involved in several pathways, including type 1 interferon (IFN) and IFNγ, NF-κB, and antigen presentation.[7] Nuclear PD-L1 also upregulates other immune checkpoint molecules, which could contribute to the resistance to anti-PD-1 therapy seen in breast cancer cells and murine colon cancer models.[7] In a melanoma model, anti-PD-1 therapy led to the accumulation of granulocytic myeloid-derived suppressor cells (MDSCs) through cell-intrinsic PD-L1/NLRP3 inflammasome signaling, which conferred acquired resistance to immunotherapy.[17] These findings imply that PD-L1's intrinsic function contributes to primary and adaptive resistance to ICIs; however, the underlying mechanisms are thus far unknown.

IL-6 is involved in cancer development and progression via tumor-cell-intrinsic and tumor-cell-extrinsic pathways. In addition to supporting cancer cell proliferation and survival, as well as tumor angiogenesis and invasion,[18 19] it is involved in shaping the immunosuppressive tumor microenvironment (TME) by inhibiting dendritic cell function, skewing CD4 T-cell differentiation from Th1 into Tregs, polarizing macrophages into the M2 type, and promoting the generation and activation of MDSCs.[18 20–24] IL-6 also increases T-cell proliferation and survival while activating antitumor T-cell responses by recruiting CD8 T-cells to lymph nodes and tumor sites.[19 20 25] These conflicting roles of IL-6 might be due to the cellular source of IL-6, the type of IL-6 signaling, the stage of the immune response, the tumor type, and other contextual variables.[18–20] However, regulation of the IL-6 pathway in cancer and the role of IL-6 in cancer immunotherapy are not fully understood, particularly regarding intrinsic PD-L1 function.

This study investigated the mechanisms by which intrinsic PD-L1 function suppresses antitumor immunity and thus drives resistance to ICIs. Our results show that tumor cell-intrinsic PD-L1 activates the IL-6/Jak/Stat3 pathway, thereby contributing to the recruitment and activation of MDSCs, the suppression of antitumor immunity, and resistance to ICI in PD-L1-high NSCLC.

METHODS

Patient cohorts with ICI therapy

Three cohorts of patients with NSCLC receiving ICI therapy (PD-1 or PD-L1 blockade) were included in this study (online supplemental tables S1–S3). In the ICI–RNA-sequencing (ICI-RNS-seq) cohort (n=234), tumor tissues from patients with NSCLC obtained before ICI therapy were subjected to RNA-seq as described in online supplemental methods. Using the RNA-seq data, gene set enrichment analysis (GSEA) and immune cell abundance analysis were performed as described in online supplemental methods. In the ICI-serum cohort (n=57), serum samples taken before ICI therapy were analyzed for IL-6 using ELISA. In the ICI–immunohistochemistry (ICI-IHC) cohort (n=71), resected tumor tissues before ICI therapy were subjected to IHC. Treatment response was evaluated according to RECIST V.1.1, and clinical outcomes were defined as described in online supplemental methods.

Public database analysis

Level 3 RNA-seq data of NSCLC from The Cancer Genome Atlas (TCGA) were downloaded from the GDC portal (http://portal.gdc.cancer.gov/) using the "TCGABiolinks" R-package. TCGA datasets were analyzed using GSEA software (V.4.2.3), MSigDB (Broad Institute), and the CIBERSORTx algorithm (http://cibersortx.stanford.edu/). The MDSC signature score was defined as the mean z-score of the $\log_2$(fold-change) among all genes listed in online supplemental table S4. Gene expression data in human lung cancer cell lines were downloaded from the Cancer Cell Line Encyclopedia (CCLE) website (https://portals.broadinstitute.org/ccle).

Cell lines and reagents

The human NSCLC cell lines and murine lung cancer cell lines were cultured as described in online supplemental methods. Reagents and neutralizing antibodies used throughout the experiments are detailed in online supplemental table S5 or the corresponding methods section.

Primary lung cancer cells and analysis of lung tumors

Resected patient lung cancer tissues were dissociated with collagenase IV (0.5 mg/mL; Sigma-Aldrich). Single tumor cells were filtered through a 70 µm pore cell strainer and treated with red blood cell lysis buffer. CD45-negative cells, sorted by FACS using FACSAria-III (BD Biosciences), were seeded in six-well plates coated with poly-L-lysine (Sigma-Aldrich), cultured in RPMI-1640 (Biowest) supplemented with 10% fetal bovine serum and antibiotics, and transfected with a PD-L1 plasmid vector or small interfering RNAs (siRNAs). In addition, single tumor cells were analyzed by flow cytometry to identify the MDSC population.

Transfection of expression vectors and siRNAs

Human PD-L1-expressing plasmids (HG10084-UT), PD-L1-Flag-tagged plasmids (HG10084-NF), control vectors (CV020), and human protein tyrosine phosphatase 1B (PTP1B)-Myc-tagged plasmids (HG10304-CM) were purchased from Sino Biological (China). siRNAs targeting human PD-L1 (NM 014143.2) were designed and synthesized by Bioneer (Republic of Korea) with the following sequences: sense 5′-CUG AGA AUC AAC ACA ACA A (dTdT)-3′ and antisense 5′-UUG UUG UGU UGA UUC UCA G (dTdT)-3′. Plasmid vectors and siRNAs were transfected using the jetPRIME transfection reagent (Polyplus) according to the manufacturer's instructions.

RNA-seq of cell lines

A549 cells with PD-L1 overexpression and H460 cells with PD-L1 knockdown were submitted to RNA-seq as described in online supplemental methods.

Generation of mouse stable cell lines

Mouse Lewis lung carcinoma (LLC) cells with stable PD-L1 overexpression or knockdown were generated as described in online supplemental methods.

IHC and immunofluorescence staining

IHC and immunofluorescence staining were performed using the antibodies listed in online supplemental table S6 as described in online supplemental methods.

Co-immunoprecipitation and western blotting

Co-immunoprecipitation and western blotting were performed using whole cell lysates or after cellular fractionation using the antibodies listed in online supplemental table S6 as described in online supplemental methods.

Flow cytometry

Flow cytometry was performed using the antibodies listed in online supplemental table S7 as described in online supplemental methods.

ELISA

Cytokines in the culture supernatants were measured using the ELISA kits listed in online supplemental table S8 in accordance with the manufacturers' instructions.

Quantitative real-time reverse-transcription PCR

Total mRNA was extracted from cells and tumor tissues and submitted to Quantitative real-time reverse-transcription PCR (qRT-PCR) using the primers listed in online supplemental table S9 as described in online supplemental methods.

Pull-down assay

A glutathione S-transferase pull-down assay was performed to evaluate the binding between PD-L1 and PTP1B as described in the online supplemental methods.

PTP1B phosphatase assay

PTP1B activity was measured using two different assays as detailed in online supplemental methods.

Luciferase reporter assay

An IL-6 luciferase reporter assay was performed as described in online supplemental methods.

Duolink proximity ligation assay

Interactions between PD-L1 and phosphorylated Stat3 (p-Stat3) were detected by performing a proximity ligation assay with a Duolink In Situ Red Starter Kit (Sigma-Aldrich) as described in online supplemental methods.

The CUT&Tag assay was performed according to the EpiCypher CUTANA CUT&Tag Protocol V.1.7. The sequencing data were analyzed as described in online supplemental methods.

Chromatin immunoprecipitation-qPCR

A chromatin immunoprecipitation (ChIP) assay was performed with a Pierce Magnetic ChIP Kit (Thermo Fisher Scientific) using the antibodies listed in online supplemental table S6 as described in online supplemental methods. Immunoprecipitated DNA fragments were eluted from the magnetic beads and assessed by qPCR using the primers listed in online supplemental table S10.

In vitro co-culture of human MDSCs and cancer cells

Human peripheral blood mononuclear cells (PBMCs) were isolated from healthy donors. Ficoll gradient separation was used to isolate polymorphonuclear (PMN)-MDSCs and neutrophils. PMN-MDSCs were enriched in the low-density fraction (mononuclear cell layer), while most neutrophils were enriched in the high-density fraction (leukocyte layer). The low-density fraction was further purified and sorted using FACSAria-III (online supplemental figure S8A). HLA-DR^{lo}CD11b^{+}CD33^{+}CD14^{+} cells/HLA-DR^{lo}CD11b^{+}CD33^{+}CD15^{+} cells/and CD15+low-density neutrophils were together submitted to co-culture experiments as "human MDSCs". Cancer cells transfected with PD-L1-overexpressing vectors or PD-L1 siRNAs were seeded in the lower chamber of a 0.4 µm pore Transwell system (SPL Life Sciences) 24 hours after their transfection, and MDSCs were seeded in the upper chamber. After 4 days of co-culture in the presence of granulocyte macrophage colony-stimulating factor

(GM-CSF) (20 ng/mL), cytokine concentrations in the culture supernatants were measured by ELISA, and the MDSCs were subjected to qRT-PCR or subsequently co-cultured with T-cells.

Migration of MDSCs co-cultured with cancer cells or their conditioned medium (CM) was detected as described in online supplemental methods.

T-cell proliferation and Treg differentiation assays

Human $CD4^+$ and $CD8^+$ T-cells were isolated from PBMCs of healthy donors using FACSAria-III, stained with 1 µM carboxyfluorescein succinimidyl ester (CFSE) (Invitrogen), and stimulated with anti-CD3/CD28 beads (Thermo Fisher Scientific). The T-cells were then co-cultured with MDSCs (T-cell:MDSC=5:1), that had been incubated with cancer cells or their CM on the opposite sides of a 0.4 µm pore Transwell system. After 72 hours of co-culture, CFSE-labeled T-cells were assessed by flow cytometry for T-cell proliferation. $CD4^+$ T-cells were evaluated for Treg differentiation by flow cytometry.

Cell apoptosis assay

$CD8^+$ tumor-infiltrating lymphocytes were isolated from mouse tumor tissue using CD8-specific microbeads (Miltenyi Biotec) and co-cultured with CFSE-labeled LLC cells (E:T=5:1) for 24 hours. The cells were stained with 7-AAD and Annexin V-PE and analyzed by flow cytometry.

Animal studies

Wild-type female C57BL/6 mice, aged 6–7 weeks, were purchased from Orient Bio (Republic of Korea), and Pdcd1-knockout mice were purchased from Jackson Laboratory (USA).

The mice were randomly allocated to different experimental groups (n=5 per group). Mouse cell lines (5×10^5 cells/mouse) were subcutaneously injected into the flanks of syngeneic C57BL/6 mice. Tumor size was measured every 2–3 days using calipers and calculated as tumor volume using the following formula: tumor volume (mm^3)=(length×$width^2$)/2. The neutralizing/blocking antibodies and isotype controls used for the in vivo experiments are listed in online supplemental table S5, and their administration schedules are in the figure legends. Before the mice were euthanized, tumor size was measured using an IVIS Spectrum imaging system (PerkinElmer).

Isolation of mouse myeloid cells from spleen for co-injection with tumor cells

For the MDSC and LLC tumor cell co-injection experiments, $CD11b^+Ly6G^+$ and $CD11b^+Ly6C^+$ myeloid cells were isolated from the spleens of tumor-free (naïve) C57BL/6 mice using FACSAria-III. The isolated cells were cultured for 48 hours in CM of PD-L1-overexpressing or PD-L1-knockdown LLC cells supplemented with 20 ng/mL GM-CSF and then co-injected with wild-type LLC cells into the flanks of the mice at a 1:3 ratio.

Isolation of mouse MDSCs from tumor tissue and T-cell suppression assay

Mouse MDSCs were isolated from tumor tissue using an MDSC isolation kit (Miltenyi Biotec). $CD8^+$ T-cells were isolated from tumor-free (naïve) mouse spleen using FACSAria-III. CFSE-labeled T-cells were stimulated with anti-CD3/CD28 beads (Thermo Fisher Scientific) and co-cultured for 72 hours with the tumor-derived MDSCs in a 0.4 µm pore Transwell system. T-cell proliferation was assessed by flow cytometry.

Statistical analysis

The data were analyzed using GraphPad Prism V.10.2.2 statistical software (USA) as described in online supplemental methods. A two-sided $p<0.05$ was considered statistically significant.

RESULTS

IL-6 predicts a poor response to ICI therapy in PD-L1-high NSCLC

To explore the mechanism of unresponsiveness to ICIs in PD-L1-high NSCLC, the ICI-RNA-seq cohort was analyzed (dataset available in the Gene Expression Omnibus database, accession number GSE285029). GSEA of the RNA-seq data revealed that in the *CD274* (PD-L1)-low group, the IL-6/Jak/Stat3 pathway was enriched among ICI responders (partial response, PR) compared with non-responders (stable disease (SD)+progressive disease (PD)) (figure 1A). By contrast, in the *CD274*-high group, the IL-6/Jak/Stat3 pathway was enriched in non-responders (figure 1B). A heatmap of the genes in the core enrichment site of the IL-6/Jak/Stat3 pathway showed that *IL6* was one of the most highly differentially expressed genes (DEGs) between responders and non-responders in the *CD274*-high group (figure 1C). *IL6* expression levels were higher in patients with progressive disease in the *CD274*-high group (figure 1D). Whereas high *CD274* expression predicted better responses and clinical outcomes, high *IL6* expression was significantly associated with poor responses and clinical outcomes in the *CD274*-high group but not in the *CD274*-low group (figure 1E,F). Immune cell signature scoring revealed decreases in cytotoxic T-lymphocytes (CTLs) and increases in MDSCs in non-responders in the *CD274*-high group (figure 1G,H). *IL6* expression correlated positively with the Treg and MDSC scores in non-responders in the PD-L1-high group (figure 1H).

In the ICI-serum cohort, PD-L1 expression (tumor proportion score (TPS)) correlated positively with serum IL-6 levels, particularly in patients with progressive disease (figure 1I). Patients with high serum IL-6 levels had a poor response and shorter survival after ICI therapy (figure 1J,K).

These findings imply that IL-6 is associated with an immunosuppressive TME and a poor response to ICI therapy in PD-L1-high NSCLC.

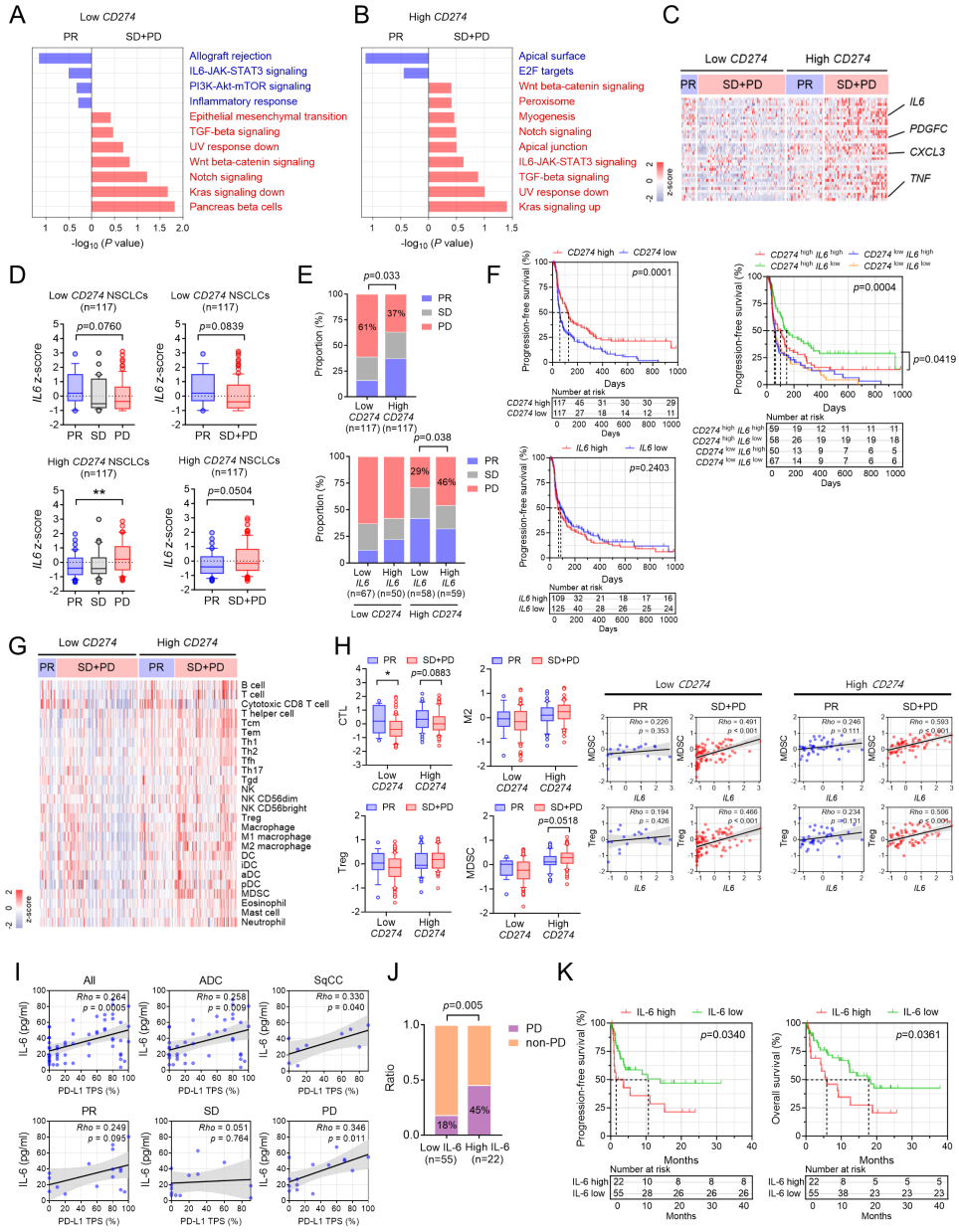

Figure 1 IL-6 predicts a poor response to ICI therapy in patients with PD-L1-high NSCLC. (A, B) Tumor tissues from 234 patients with NSCLC before ICI therapy were subjected to RNA-seq. The patients were divided into low-*CD274* and high-*CD274* (PD-L1) groups based on the median value. Differences in pathway enrichment between responders with a partial response (PR) and non-responders with stable disease (SD) or progressive disease (PD) in each group were analyzed using GSEA. (C) The heatmap shows the relative mRNA expression levels of the genes in core enrichment sites of the IL-6/Jak/Stat3 gene set. (D) Differences in *IL6* expression (as presented as z-scores) among patients with PR, SD, and PD or between those with PR and SD+PD in the low-*CD274* and high-*CD274* groups. (E) ICI responsiveness among patients divided into low-expression and high-expression groups for *CD274* and *IL6*, based on the median value for *CD274* and a TPM cut-off of 1.805 for *IL6*, as determined using Cutoff Finder software. Differences in the response rate were compared using Pearson's $\chi 2$ test. (F) Kaplan-Meier analysis of progression-free survival (PFS) after ICI therapy was performed according to *CD274* (left upper), *IL6* (left lower), and combined *CD274* and *IL6* (right) expression. Survival differences were compared using a log-rank test. (G) The heatmap shows the relative immune cell abundance of each group. (H) Differences in CTL, M2 macrophage, Treg, and MDSC scores between patients with PR and SD+PD in the low-*CD274* and high-*CD274* groups. Correlations between MDSC and Treg scores and *IL-6* expression among patients with PR and SD+PD in the low-PD-L1 and high-PD-L1 groups. (I) Correlations between serum IL-6 levels and PD-L1 expression determined by the TPS of PD-L1 (22C3) IHC in the ICI-serum cohort (n=57). (J) The proportions of patients with PD and non-PD in the low-serum and high-serum IL-6 groups (cut-off value estimated using Cutoff Finder software) were compared using Pearson's chi-squared test. (K) Kaplan-Meier analysis of PFS and overall survival (OS) after ICI therapy according to serum IL-6 levels. Differences in survival were analyzed using a log-rank test. The data in the histogram are presented as means±SEM. Correlations were calculated using Spearman's correlation test. *p<0.05, **p<0.01. ADC, adenocarcinoma; ICI, immune checkpoint inhibitor; MNSCLC, non-small-cell lung cancer; DSC, myeloid-derived suppressor cell; SqCC, squamous cell carcinoma.

PD-L1 overexpression activates the IL-6/Jak2/Stat3 pathway in lung cancer cells

To determine the relationship between IL-6 and PD-L1 in NSCLC, TCGA data were analyzed. The IL-6/Jak/Stat3 pathway was enriched in PD-L1-high tumors (online supplemental figure S1A,B). To investigate the cell-intrinsic role of PD-L1 in the IL-6/Jak/Stat3 pathway, NSCLC cell lines were screened for basal PD-L1 expression. A549 and H522 cells, which have low basal PD-L1 expression, were transfected with a PD-L1-overexpression vector, while H460 and H596 cells, which have high basal PD-L1 expression, were transfected with PD-L1 siRNA (online supplemental figure S1C–E). The cells were then submitted to RNA-seq and in vitro analyses. Among the DEGs identified in RNA-seq, 359 genes were upregulated on PD-L1 overexpression in A549 cells and downregulated on PD-L1 knockdown in H460 cells, including *IL6* (figure 2A–C). In GSEA using DEGs, the IL-6/Jak/Stat3 pathway was increased in PD-L1-overexpressing A549 cells and decreased in PD-L1-knockdown H460 cells (figure 2D,E).

Among the cytokines and chemokines from the IL-6/Jak/Stat3 gene set[26] regulated by PD-L1 (figure 2F), the expression and production of several cytokines (ie, *IL6*, *TNF*, *TGFB1*, *IL1B*) and chemokines (ie, *CXCL1*, *CXCL3*, and *CXCL8*) after PD-L1 overexpression and knockdown in NSCLC cells were validated using qRT-PCR and ELISA (figure 2G; online supplemental figure S2A,B). For primary lung cancer cell culture and transfection, CD45-negative cells were sorted by FACS from resected tumor tissues of patients with PD-L1-low NSCLC (TPS<1, n=5) and PD-L1-high NSCLC (TPS≥50, n=3) (online supplemental figure S2C). In cultures of primary lung cancer cells, the levels of these cytokines and chemokines in the culture supernatants were higher in PD-L1-high tumors than in PD-L1-low tumors, and they increased by PD-L1 overexpression and decreased by PD-L1 knockdown (figure 2H; online supplemental figure S2C,D). IL-6 expression, phosphorylated Jak2 and Stat3, and the nuclear translocation of p-Stat3 increased by PD-L1 overexpression and decreased by PD-L1 knockdown (figure 2I,J). The increase in cytokine expression by PD-L1 overexpression was blocked by Jak2 and Stat3 inhibitors (online supplemental figure S2E). In the NSCLC cell lines from CCLE, *CD274* expression correlated positively with *JAK2*, *STAT3*, and *IL6* expression (online supplemental figure S3). Together, these results imply that tumor-cell-intrinsic PD-L1 increases the expression of the above-mentioned cytokines and chemokines in NSCLC through Jak2/Stat3 activation.

PD-L1 overexpression in response to IFNγ increased p-Jak2 and p-Stat3 levels, as well as IL-6 expression, in A549 and H522 cells; this effect was diminished by PD-L1 knockdown (online supplemental figure S4A). In addition, recombinant PD-1 stimulated cytokine and chemokine production in H460 and H596 cells, but this response was suppressed in PD-L1-knockdown cells (online supplemental figure S4B). These findings imply that PD-L1-dependent activation of the Jak2/Stat3/IL-6 pathway may occur within the lung cancer microenvironment.

PD-L1 upregulates the phosphorylation of Jak2 and Stat3 by binding directly to PTP1B and inhibiting it

The mechanism by which PD-L1 activates Jak2/Stat3 was investigated by examining the proteins that can interact with PD-L1. A previous study showed that PTP1B binds to PD-L1 in MDA-MB-231 cells,[27] and PTP1B interacts with—and dephosphorylates—Jak2.[28] In HEK293T cells, Flag-tagged PD-L1 and Myc-tagged PTP1B were co-immunoprecipitated (online supplemental figure S5A). The interaction of endogenous PTP1B and PD-L1 in PD-L1-high H460 cells was inhibited by PD-L1 knockdown, whereas their binding increased in PD-L1-overexpressing A549 cells (online supplemental figure S5B,C). A pull-down assay showed that PTP1B interacted directly with the cytoplasmic domain of PD-L1 (online supplemental figure S5D). In an in vitro phosphatase assay using recombinant p-Jak2 as the substrate and in a PTP1B phosphatase activity assay, PD-L1 inhibited PTP1B activity (online supplemental figure S5E,F). PTP1B inhibitor restored Jak2/Stat3 phosphorylation and *IL6* transcription in PD-L1-knockdown H460 and H596 cells (online supplemental figure S5G,H). These results indicate that PD-L1 binds to and inhibits PTP1B, thus enhancing Jak2/Stat3 activity and IL-6 expression.

Nuclear PD-L1 binds to p-Stat3 and enhances its transcription efficiency for IL-6

The intrinsic role of PD-L1 in Stat3 signaling was investigated by focusing on PD-L1 localization. Nuclear localization of PD-L1 was observed in PD-L1-high NSCLC cells (figure 3A,B). Co-immunoprecipitation and Duolink assays revealed the physical interaction of PD-L1 and p-Y705-Stat3 in both the nucleus and cytosol, with a higher interaction in the nucleus of PD-L1-overexpressing cells (figure 3C,D).

A CUT&Tag assay using H460 cells showed that nuclear PD-L1-binding sites were distributed near the transcription start site (figure 3E). Well-defined overlapping peaks in the *IL6* and *CXCL1* promoters were observed in the CUT&Tag data for PD-L1 and p-Stat3 (figure 3F). In the p-Stat3 CUT&Tag assay, the genome-wide binding intensity of p-Stat3 was compromised, and enrichment of p-Stat3 in the *IL6* and *CXCL1* promoters was attenuated in PD-L1-knockdown cells (figure 3G,H). These results imply that nuclear PD-L1 localizes to the *IL6* and *CXCL1* promoter, acting as a coactivator of their transcription by p-Stat3. This role of nuclear PD-L1 was supported by the sequential ChIP-qPCR, which showed that the binding of p-Y705-Stat3 to the cytokine and chemokine promoters decreased in PD-L1-knockdown cells (figure 3I; online supplemental figure S6).

PD-L1 promotes migration and activation of MDSCs in an IL-6-dependent manner

We hypothesized that increased expression of the above cytokines and chemokines by tumor-cell-intrinsic PD-L1

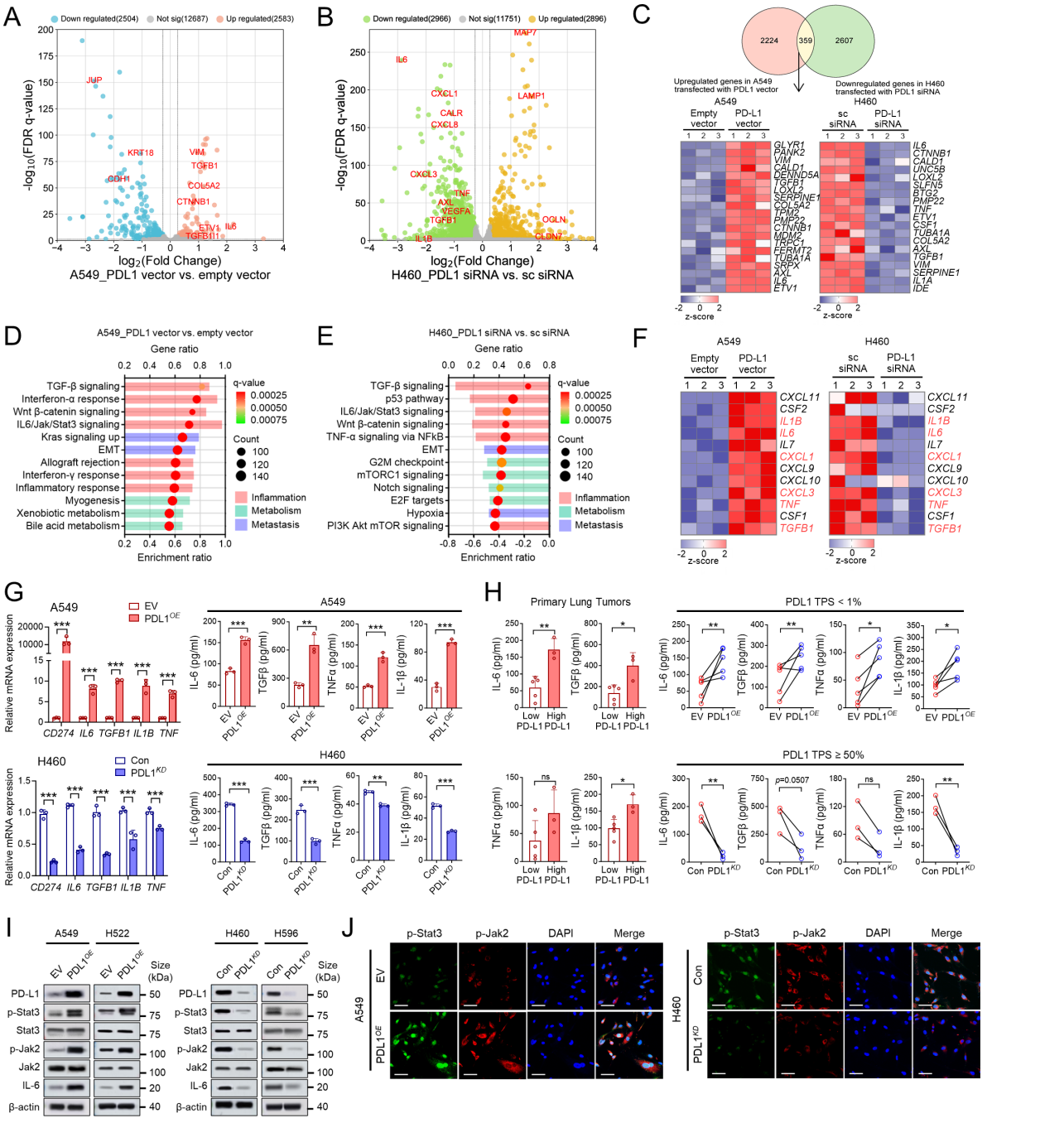

Figure 2 PD-L1 activates the IL-6/Jak2/Stat3 pathway in lung cancer cells. (A, B) RNA-seq was performed in A549 cells transfected with PD-L1 vector or empty vector and in H460 cells transfected with PD-L1 siRNA or scrambled (sc) siRNA. DEGs in PD-L1-overexpressing A549 cells and PD-L1-knockdown H460 cells are displayed in a volcano plot. (C) Venn diagram illustrating the numbers of up-regulated genes in PD-L1-overexpressing A549 cells and down-regulated genes in PD-L1-knockdown H460 cells. Of the 359 shared genes, the expression of representative genes as determined in triplicate RNA-seq experiments with both cell lines is displayed in a heatmap. (D, E) GSEA was performed in each cell line using DEGs and the Hallmark gene set. (F) Expression of representative cytokines and chemokines included in the IL-6/Jak/Stat3 gene set as determined in triplicate RNA-seq experiments with both cell lines (molecules validated by further in vitro analyses are shown in red). (G) Cytokine mRNA expression and secretion were measured by qRT-PCR and ELISA, respectively, in PD-L1-overexpressing ($PDL1^{OE}$) A549 cells and PD-L1-knockdown ($PDL1^{KD}$) H460 cells (EV, empty vector; Con, scrambled siRNA). (H) Cytokine secretion determined by ELISA in the culture supernatant of patient-derived primary human lung tumor (cancer) cells with low-PD-L1 expression (TPS<1, n=5) and high-PD-L1 expression (TPS≥50, n=3) (left). Primary lung cancer cells with low and high PD-L1 expression were transfected with PD-L1-overexpressing vector and PD-L1-knockdown siRNA, respectively, and cytokine secretion was measured by ELISA (right). (I, J) Phosphorylated Stat3 and Jak2 and IL-6 expression were detected using western blotting and immunofluorescence staining in PD-L1-overexpressing A549 and H522 cells and in PD-L1-knockdown H460 and H596 cells (scale bar=20 µm). The data in the histogram are presented as means ±SEM. *p<0.05, **p<0.01, ***p<0.001. DEGs, differentially expressed genes.

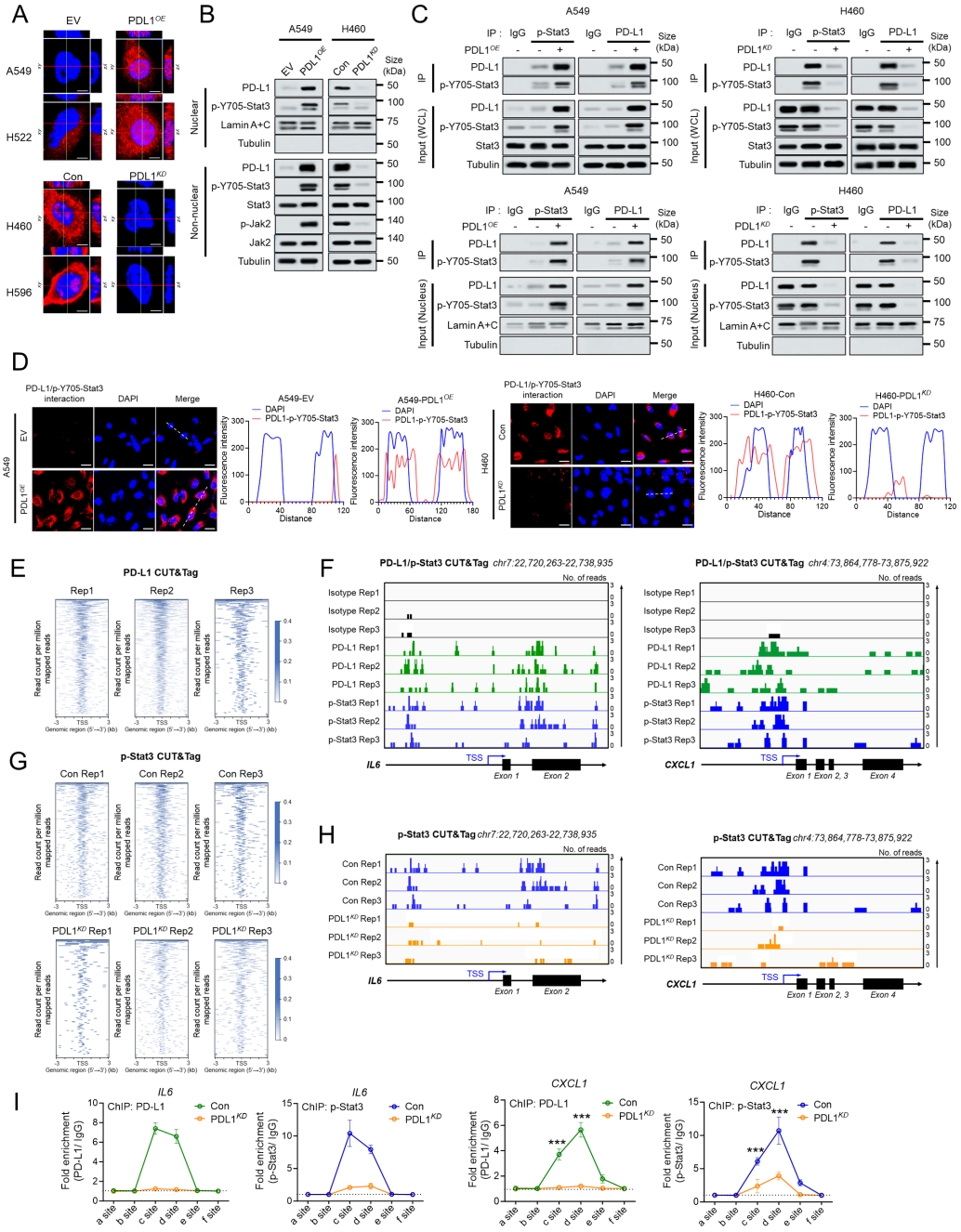

Figure 3 PD-L1 binds to p-Stat3 in the nucleus and enhances its efficiency in IL-6 transcription. (A) Three-dimensional visualization of nuclear PD-L1. Images corresponding to x-z sections reconstructed along the red lines are displayed at the top of each x-y section. Images corresponding to y-z sections reconstructed along the green solid lines are displayed at the right of each x-y section (scale bar=10 µm). (B) Nuclear localization of PD-L1 and p-Y705-Stat3 assessed by western blotting after cellular fractionation into nuclear and non-nuclear fractions, in PD-L1-overexpressing A549 cells and PD-L1-knockdown H460 cells. (C) Co-immunoprecipitation assay for p-Y705-Stat3 and PD-L1 using whole cell lysates (upper panels) and nuclear extracts (lower panels) of PD-L1-overexpressing A549 cells and PD-L1-knockdown H460 cells. (D) Interaction between p-Y705-Stat3 and PD-L1 in the cytoplasm and nucleus visualized in a Duolink assay of PD-L1-overexpressing A549 cells and PD-L1-knockdown H460 cells (scale bar=10 µm). Red dots indicate the interaction between p-Y705-Stat3 and PD-L1. Fluorescence intensity across dotted lines is depicted in the red lines of the right graphs (DAPI in blue lines). (E) A density heatmap of PD-L1 CUT&Tag sequencing data using H460 cells shows PD-L1 enrichment within 3 kb around the transcription start site (TSS) (Rep, replica). (F) Integrative genomics viewer (IGV) tracks for *IL6* and *CXCL1* promoters from the PD-L1 and p-Stat3 CUT&Tag analyses. (G) The density heatmap of the p-Stat3 CUT&Tag data shows compromised p-Stat3 enrichment in PD-L1-knockdown H460 cells vs control cells within 3 kb around the TSS. (H) IGV tracks for *IL6* and *CXCL1* promoters from the p-STAT3 CUT&Tag analysis of PD-L1-knockdown H460 cells and control cells. (I) Chromatin immunoprecipitation (ChIP) was performed using anti-PD-L1 and anti-Y705-Stat3 antibodies in PD-L1-knockdown H460 cells. The binding of PD-L1 and p-Y705-Stat3 to the *IL6* and *CXCL1* promoters was then assessed by qPCR (sequential ChIP-qPCR). The data are presented as the mean±SEM of three independent experiments. ***p<0.001.

would affect antitumor immunity. Because there was no significant difference in the 22 immune cell fractions between PD-L1-low and PD-L1-high NSCLCs in the CIBERSORTx analysis of the TCGA data (online supplemental figure S7A,B), we focused on MDSCs, which are not included in CIBERSORTx. Expression of the 40 signature genes of MDSCs (online supplemental table S4) was generally elevated in PD-L1-high NSCLC (figure 4A). MDSC scores correlated positively with *CD274* expression and with the expression of the cytokines and chemokines increased by PD-L1 (figure 4B; online supplemental figure S7C,D). Moreover, in a FACS analysis of patients' tumors (online supplemental figure S7E), the numbers of tumor-infiltrating monocytic MDSCs (M-MDSCs) and PMN-MDSC correlated positively with PD-L1 expression (figure 4C). These findings imply that intrinsic PD-L1 function may affect MDSCs via the IL-6/Jak2/Stat3 pathway, which was investigated using a mixture of HLA-DR^{lo}CD11b^{+}CD33^{+}CD14^{+} (M-MDSCs) and HLA-DR^{lo}CD11b^{+}CD33^{+}CD15^{+} cells (PMN-MDSCs) and CD15^{+} low density neutrophils (together designated as "human MDSCs" hereafter and relating figures) and T-cells sorted from PBMCs of healthy donors (online supplemental figure S8A,B).

The migration of MDSCs through the Transwell system increased when co-cultured with PD-L1-high NSCLC cells or when cultured in CM from PD-L1-overexpressing primary lung cancer cells; migration was significantly inhibited by CXCL1-neutralizing antibodies (figure 4D–G; online supplemental figure S8C). In MDSCs co-cultured with NSCLC cells in a 0.4 µm pore Transwell system, the expression of genes responsible for the suppressive function of MDSCs, including *ARG1*, *iNOS*, *TGFB1*, *IDO1*, and *IL10*, increased when co-cultured with PD-L1-overexpressing A549 cells and decreased when co-cultured with PD-L1-knockdown H460 cells (online supplemental figure S8D). In co-cultures with MDSCs previously incubated with PD-L1-high NSCLC cells, proliferation of CD4^{+} and CD8^{+} T-cells was reduced while Treg differentiation of CD4^{+} T-cells was enhanced (online supplemental figure S8E–G). The suppressive activity of MDSCs co-cultured with PD-L1-overexpressing A549 cells was significantly restored when the co-cultures were treated with IL-6-neutralizing antibodies (figure 4H,I; online supplemental figure S8G,H).

Similarly, *IDO1*, *Arg1*, and *iNOS* expression was higher in MDSCs cultured in CM from PD-L1-high or PD-L1-overexpressing primary lung cancer cells, and this response was blocked by IL-6 neutralization (figure 4J–L).

The decrease in CD8^{+} T-cell proliferation induced by MDSCs co-cultured with PD-L1-overexpressing A549 cells or cultured in CM from PD-L1-overexpressing primary lung cancer cells was restored by ARG1 and iNOS inhibitors (figure 4M). Together, these findings imply that the tumor-cell-intrinsic function of PD-L1 promotes the recruitment and suppressive activity of MDSCs in an IL-6-dependent manner.

PD-L1's intrinsic function enhances tumor growth in vivo by IL-6-mediated immunosuppression, independently of PD-1

To validate the above in vitro findings in vivo, LLC cells with stable PD-L1 overexpression or knockdown were generated (online supplemental figure S9) and subcutaneously transplanted into the flanks of C57BL/6 mice. PD-L1 overexpression in LLC cells promoted tumor growth, increased tumor-infiltrating M-MDSC and PMN-MDSC populations as well as IL-10^{+} or iNOS^{+} M-MDSCs and PMN-MDSCs, and decreased infiltration of granzyme B (GzmB)$^{+}$ or IFNγ^{+} CD8^{+} T-cells (online supplemental figure S10A–D). MDSCs isolated from PD-L1-overexpressing tumors efficiently suppressed the proliferation of CD8^{+} T-cells isolated from tumor-free mouse spleen (online supplemental figure S10E). The opposite effects were observed in PD-L1-knockdown tumors (online supplemental figure S10F–M). Tumor-infiltrating CD8^{+} T-cells isolated from the latter effectively killed LLC cells in vitro (online supplemental figure S10N).

To determine whether tumor PD-L1 promotes LLC tumor growth via MDSC and IL-6, anti-Gr-1 (Ly6C/Ly6G) antibody and anti-IL-6 antibody were administered to the mice (figure 5A,E; online supplemental figure S11A). MDSC depletion significantly decreased PD-L1-induced tumor growth; restored and increased GzmB^{+}, IFNγ^{+}, or proliferative CD8^{+} T-cells; and decreased Tregs in PD-L1-overexpressing tumors (figure 5B–D). IL-6 blockade in PD-L1-overexpressing tumors compromised tumor growth, reduced MDSC recruitment and activation, and increased the number of GzmB^{+} or IFNγ^{+} CD8^{+} T-cells (figure 5F–J,L). MDSCs isolated from tumors with IL-6 blockade were less effective in suppressing CD8^{+} T-cell proliferation (figure 5K).

To demonstrate that tumor-cell-intrinsic PD-L1 promotes tumor progression via IL-6-induced immunosuppression independently of PD-1 ligation, in vivo experiments were performed using PD-1 (*PDCD1*)-knockout mice. PD-L1 overexpression increased tumor growth, increased the recruitment and activation of MDSCs, and decreased CD8^{+} T-cell proliferation and cytotoxicity, all of which were restored by IL-6 blockade (figure 5M–R). These results imply that tumor-cell-intrinsic PD-L1 increases tumor progression via IL-6-induced immunosuppression through MDSCs, independently of PD-1.

IL-6 secreted by PD-L1-overexpressing cells promotes tumor growth in vivo via MDSC activation

To determine further whether MDSCs activated by IL-6 secreted from PD-L1-overexpressing cells contribute to immunosuppression and tumor progression, CD11b^{+}Ly6G^{+} and CD11b^{+}Ly6C^{+} myeloid cells isolated from the spleens of tumor-free mice were cultured in the CM from PD-L1-overexpressing LLC cells (LLC-PDL1^{OE}-CM) in the presence or absence of anti-IL-6 antibody and then injected into the flanks of mice together with fresh wild-type LLC cells (figure 6A). Tumor growth increased and increases in Tregs and decreases in GzmB^{+},

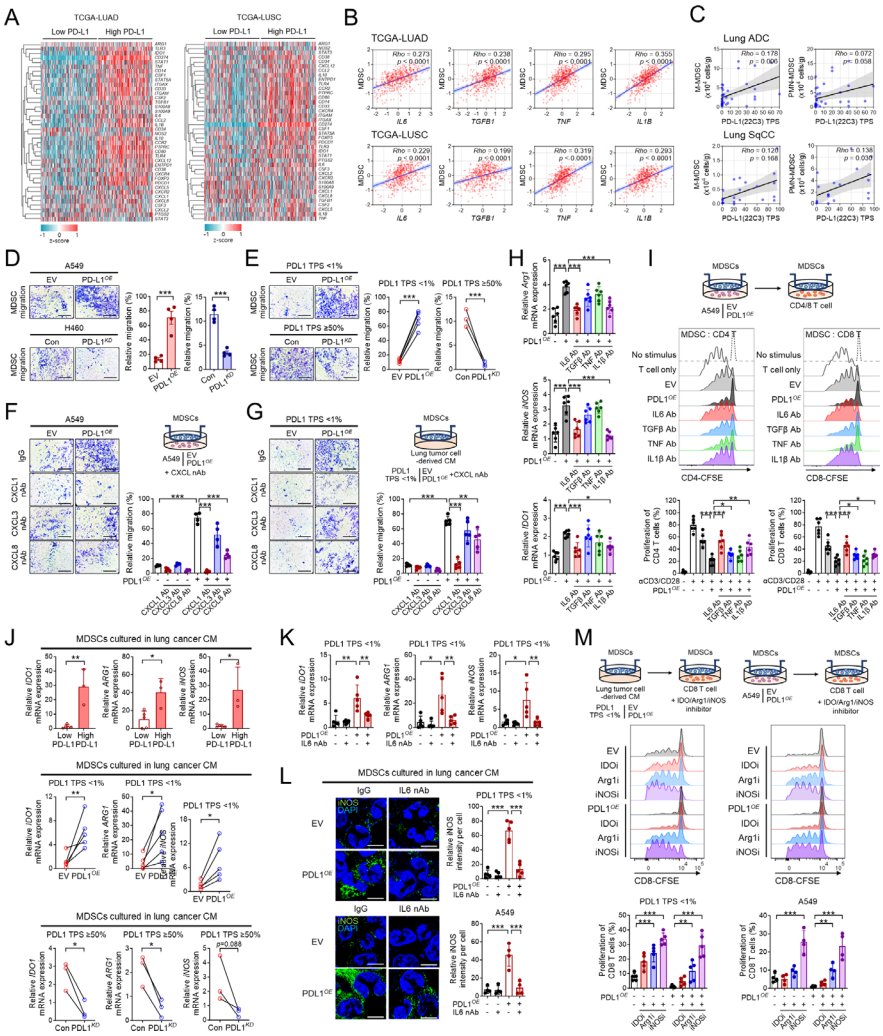

Figure 4 PD-L1 promotes CXCL1- and IL-6-dependent migration and activation of MDSCs. (A) Heatmap showing the expression of 40 MDSC signature genes in TCGA-LUAD (lung adenocarcinoma) and TCGA-LUSC (lung squamous cell carcinoma) according to PD-L1 low vs high expression (cut-off median). (B) The correlation between the MDSC score and the expression of each cytokine in TCGA-LUAD and TCGA-LUSC was calculated using Spearman's correlation test. (C) M-MDSCs and PMN-MDSCs infiltrating the tumor tissues of patients with NSCLC were analyzed by flow cytometry, and the correlation between the MDSC population and PD-L1 TPS was calculated using Spearman's correlation test. (D–M) After Ficoll gradient separation, HLA-DR^{lo}CD11b^{+}CD33^{+}CD14^{+} cells/HLA-DR^{lo}CD11b^{+}CD33^{+}CD15^{+} cells/and CD15^{+} low density neutrophils were isolated from PBMCs of healthy donors, and a mixture of these cells ("human MDSCs in figure hereafter") was submitted to in vitro assays. (D) A migration assay for human MDSCs was performed using PD-L1-overexpressing and PD-L1-knockdown NSCLC cells in an 8 µm pore Transwell system. (E) Primary lung cancer cells with low and high PD-L1 expression were transfected with PD-L1-overexpressing vector and PD-L1-knockdown siRNA, respectively. MDSC migration assays using CM from PD-L1-overexpressing and PD-L1-knockdown primary lung cancer cells were then performed. (F, G) Migration assays of MDSCs with PD-L1-overexpressing A549 cells or CM from PD-L1-overexpressing primary lung cancer cells were performed in the presence of the indicated chemokine-neutralizing antibodies (scale bar=1000 µm). (H) MDSCs were co-cultured with PD-L1-overexpressing A549 cells in a 0.4 µm pore Transwell system in the presence of the indicated cytokine-neutralizing antibodies (1 µg/mL each). *Arg1*, *iNOS*, and *IDO1* expression in MDSCs was then assessed by qRT-PCR. (I) MDSCs and PD-L1-overexpressing A549 cells were co-cultured in a 0.4 µm pore Transwell system in the presence of the indicated cytokine-neutralizing antibodies. MDSCs were then co-cultured in a 0.4 µm pore Transwell system with CFSE-labeled anti-CD3/CD28 bead-stimulated CD4^{+} or CD8^{+} T-cells; T-cell proliferation was then analyzed by flow cytometry. (J) MDSCs were cultured with CM from PD-L1-low (TPS<1) and PD-L1-high (TPS≥50) primary lung cancer cells or CM from PD-L1-overexpressing or PD-L1-knockdown primary lung cancer cells, then analyzed for *IDO1*, *Arg1*, and *iNOS* expression by qRT-PCR. (K, L) MDSCs were cultured with CM from PD-L1-overexpressing primary lung cancer cells in the presence of IL-6-neutralizing antibodies and then assessed for *IDO1*, *Arg1*, and *iNOS* expression by qRT-PCR. iNOS expression in MDSCs was detected by immunofluorescence staining (scale bar=10 µm). (M) MDSCs were cultured in CM from PD-L1-overexpressing primary lung cancer cells or co-cultured with PD-L1-overexpressing A549 cells and then co-cultured with CFSE-labeled anti-CD3/CD28 bead-stimulated CD8^{+} T-cells in the presence of the indicated inhibitors; T-cell proliferation was analyzed by flow cytometry. The data are presented as the mean±SEM of 4–6 independent experiments. *p<0.05, **p<0.01, ***p<0.001. MDSC, myeloid-derived suppressor cell; PMN, polymorphonuclear; TCGA, The Cancer Genome Atlas.

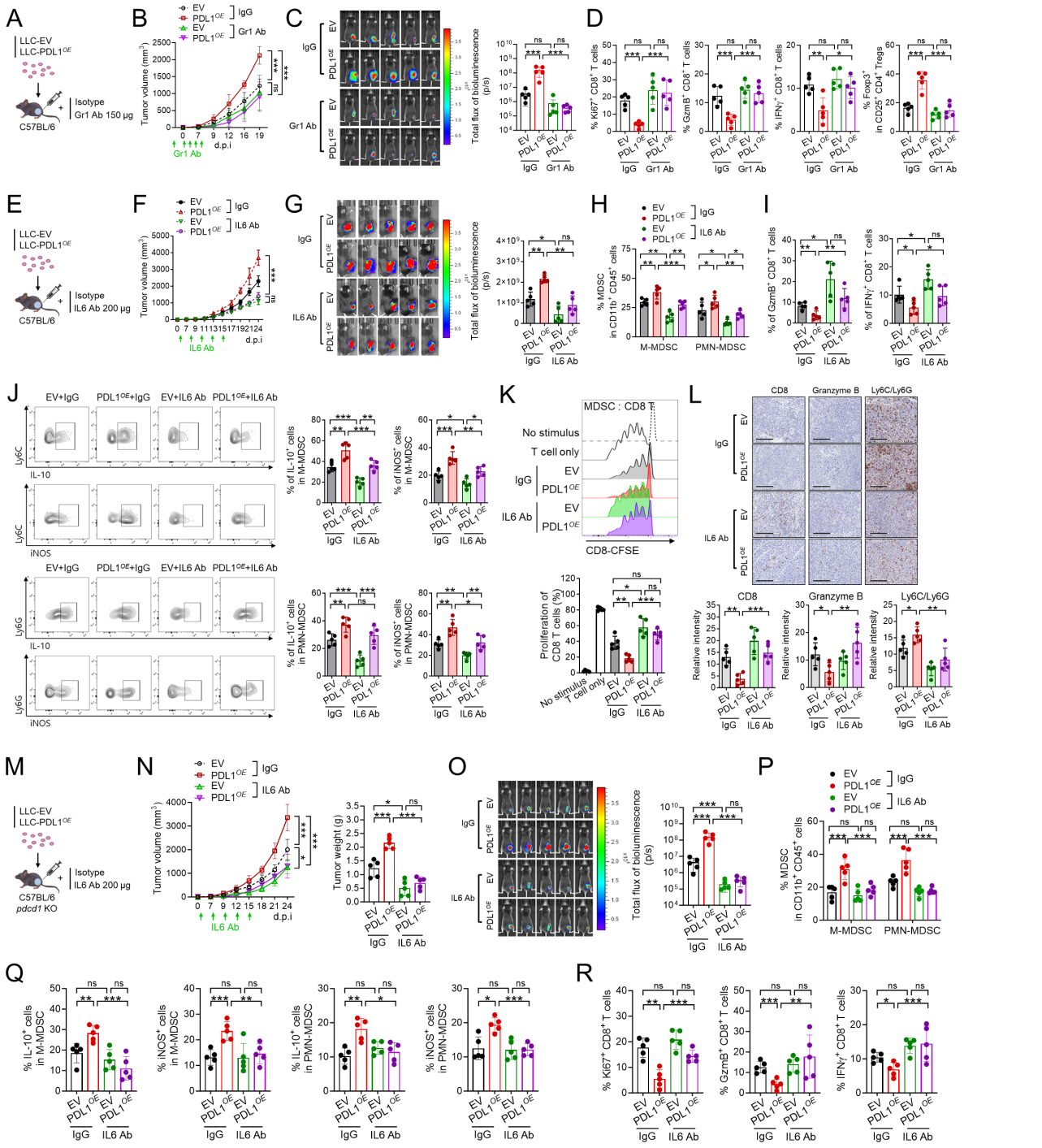

Figure 5 PD-L1 promotes tumor growth in vivo via IL-6-induced immune suppression in a PD-1-independent manner. Stable PD-L1-overexpressing LLC cells and control cells were injected subcutaneously into the flanks of C57BL/6 mice. (A–C) For MDSC depletion, mice were intraperitoneally injected with 150 µg of anti-Ly6C/Ly6G (Gr-1) antibody five times, once every 2 days, starting from 1 day before cancer cell injection. Tumor size was measured every 2–3 days using calipers. Tumor volume was measured using the IVIS luminescence imaging system before the mice were euthanized. (D) Immune cell populations in the tumors were assessed using flow cytometry. (E–G) Mice were injected intraperitoneally with 200 µg of anti-mouse IL-6 antibodies every 3 days (a total of five times). Tumor size was measured every 2–3 days using calipers. Tumor volumes were measured using the IVIS luminescence imaging system. (H–J) Immune cell populations in tumors were assessed using flow cytometry. (K) MDSCs isolated from the mouse tumors were cultured with CFSE-labeled anti-CD3/CD28 bead-stimulated $CD8^+$ T-cells isolated from the spleen of tumor-free C57BL/6 mice. T-cell proliferation was then assessed using flow cytometry. (L) IHC staining of $CD8^+$, $GzmB^+$, and $Ly6C/Ly6G^+$ cells in the tumors (scale bar=200 µm). (M–O) Stable PD-L1-overexpressing LLC cells and control cells were injected subcutaneously into the flanks of *PDCD1* (PD-1)-knockout C57BL/6 mice. Tumor size was measured once every 2–3 days using calipers. Tumor volumes were measured using the IVIS luminescence imaging system. (P–R) Immune cell populations in tumors were assessed using flow cytometry. The data are presented as the mean±SEM of five independent experiments. *p<0.05, **p<0.01, ***p<0.001. LLC, Lewis lung carcinoma; MDSC, myeloid-derived suppressor cell.

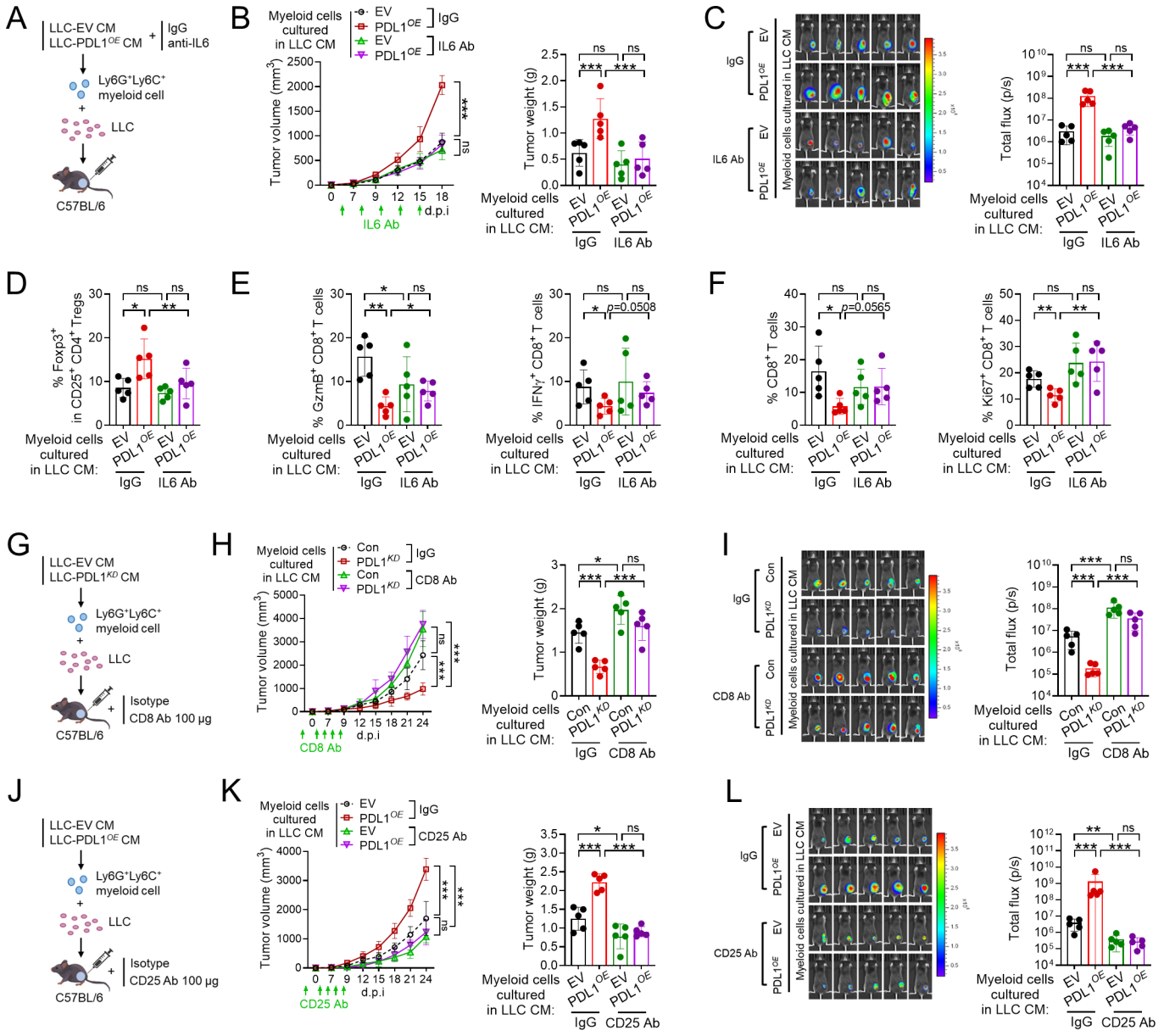

Figure 6 IL-6 secreted by PD-L1-overexpressing cells promotes tumor growth in vivo via myeloid cell activation and an immunosuppressive TME. (A) Stable PD-L1-overexpressing LLC cells and control cells were cultured for 48 hours. $CD11b^+Ly6G^+$ and $CD11b^+Ly6C^+$ myeloid cells isolated from tumor-free mouse spleens were then cultured for 48 hours in CM from PD-L1-overexpressing LLC cells (LLC-$PDL1^{OE}$-CM) in the presence or absence of IL-6-neutralizing antibodies and then injected with fresh wild-type LLC cells (at an equivalent ratio of 1:3) into the flanks of mice (EV, empty vector). (B, C) Tumor size was measured once every 2–3 days using calipers. Tumor volume was measured using the IVIS Spectrum imaging system, after which the mice were euthanized and tumor weight was determined. (D–F) Immune cell populations in the tumors were assessed using flow cytometry. (G–I) $CD11b^+Ly6G^+$ and $CD11b^+Ly6C^+$ myeloid cells isolated from tumor-free mouse spleens were cultured for 48 hours in CM from PD-L1-knockdown LLC cells (LLC-$PDL1^{KD}$-CM) and then injected with fresh wild-type LLC cells (at an equivalent ratio of 1:3) into the flanks of mice (Con, control). For $CD8^+$ T-cell depletion, the mice were intraperitoneally injected with 100 μg of anti-CD8 antibody five times, once every 2 days starting from 1 day before cancer cell injection. Tumor size was measured once every 2–3 days using calipers. Tumor size was measured using the IVIS Spectrum imaging system, after which the mice were euthanized and tumor weight was determined. (J–L) $CD11b^+Ly6G^+$ and $CD11b^+Ly6C^+$ myeloid cells isolated from tumor-free mouse spleens were cultured for 48 hours in CM from PD-L1-overexpressing LLC cells (LLC-$PDL1^{OE}$-CM) and then injected with fresh wild-type LLC cells (at an equivalent ratio of 1:3) into the flanks of mice. For Treg depletion, the mice were intraperitoneally injected with 100 μg of anti-CD25 antibody five times, once every 2 days starting from 1 day before cancer cell injection. Tumor size was measured once every 2–3 days using calipers. Tumor size was measured using the IVIS Spectrum imaging system, after which the mice were euthanized and tumor weight was determined. *p<0.05, **p<0.01, ***p<0.001. LLC, Lewis lung carcinoma.

IFNγ$^+$, or proliferative CD8$^+$ T-cells were observed in mice injected with myeloid cells cultured in LLC-PDL1^{OE}-CM plus LLC cells; these effects were reversed by the addition of anti-IL-6 Ab to the LLC-PDL1^{OE}-CM (figure 6B–F). Additionally, the reduction in tumor growth in mice injected with myeloid cells cultured in CM from PD-L1-knockdown LLC cells (LLC-PDL1^{KD}) was restored by CD8 T-cell depletion (figure 6G–I; online supplemental figure S11B). Increased tumor growth in mice injected with myeloid cells cultured in LLC-PDL1^{OE}-CM was suppressed by Treg depletion (figure 6J–L; online supplemental figure S11C). These findings imply that the immunosuppressive action of myeloid cells on adaptive T-cell immunity mediates the tumor-promoting role of myeloid cells incubated with CM of PD-L1-high LLC cells.

Moreover, the reduction in tumor growth, the decrease in MDSCs, and the increase in effector T-cells induced by IL-6 blockade were more pronounced in LLC tumors than in LLC-PDL1^{KD} tumors (online supplemental figure S11D–H). These findings support the notion that PD-L1 overexpression contributes to MDSC-mediated immunosuppression via IL-6.

Combined blockade of IL-6 and PD-1 efficiently controls tumor growth and elicits an antitumor immune response

Given that PD-L1-induced immunosuppression was restored by IL-6 blockade, the effect of combined blockade of IL-6 and PD-1 was investigated. The combined therapy efficiently suppressed tumor growth and prolonged the survival of the tumor-bearing mice (figure 7A–G). The infiltration of immunosuppressive cells, including MDSCs and Tregs, markedly decreased, whereas the infiltration of effector CD8$^+$ T-cells increased (figure 7H–M). When combined therapy was administered, MDSCs isolated from the tumors were less effective in suppressing T-cell proliferation, while CD8$^+$ T-cells isolated from the tumors were more effective in killing LLC cells (figure 7N,O). These results imply that combination therapy targeting IL-6 and PD-1 has synergistic antitumor activity by restoring the immunosuppression mediated by the PD-L1/Jak2/Stat3/IL-6/MDSC axis (figure 7P).

Finally, in the ICI-IHC cohort, the PD-L1 TPS correlated positively with IL-6 H-scores in non-responders (online supplemental figure S12A,B). In the PD-L1-high (TPS≥50) group, the response to ICI therapy and the prognosis were poorer in patients with IL-6-high tumors (online supplemental figure 12C,D). In the PD-L1-high group, the IL-6 H-scores of non-responders correlated negatively with tumor-infiltrating CD8$^+$ lymphocytes and positively with Foxp3$^+$ cells and MDSCs (CD33$^+$CD11b$^+$ cells) (online supplemental figure 12E). The MDSC IHC scores were highest in IL-6-high/PD-L1-high tumors (online supplemental figure 12F). The findings from the ICI-IHC cohort were comparable to those from the ICI-RNA-seq cohort, providing further evidence that IL-6 produced by PD-L1-high-tumor cells suppresses ICI responsiveness via MDSCs in patients with NSCLC.

DISCUSSION

MDSCs play important roles in immune evasion and tumor progression by inhibiting the antitumor function of T-cells and NK-cells and accumulating and stimulating other immunosuppressive cells via secretion of soluble factors and expression of immune checkpoint molecules.[20 29] MDSCs are of prognostic and predictive value in diverse cancers and various therapeutics and are associated with primary and acquired resistance to cancer immunotherapy.[20 29–31] In a murine lung cancer model, an E3 ligase, TRIM28, upregulated expression of CXCL1 and recruitment of MDSCs to the TME, thereby increasing resistance to anti-PD-1 therapy.[32] In other murine lung cancer models, suppression of MDSC recruitment and function by MEK and HDAC inhibitors enhanced the antitumor efficacy of anti-PD-1/PD-L1 therapy.[33 34] Thus, clinical trials targeting MDSCs in combination with ICIs have been conducted.[29 31] However, the mechanism that regulates MDSC infiltration and activity in tumors remains incompletely understood. This study demonstrated a novel immunosuppressive mechanism of tumor-cell-intrinsic PD-L1 via the Jak/Stat3/IL-6/MDSC axis.

A relationship between IL-6 and PD-L1 has been reported in several cancers previously. In hepatocellular carcinoma, IL-6/Jak1 signaling leads to PD-L1 phosphorylation and, in turn, to stabilization of PD-L1, thus promoting immune evasion.[35] IL-6 enhanced PD-L1 expression in NSCLC cells via the Jak1/Stat3 pathway and suppressed antitumor immunity, while IL-6 blockade downregulated PD-L1 expression.[36] By contrast, IL-6 was produced by macrophages of the melanoma microenvironment after ICI treatment, and IL-6 blockade increased PD-L1 expression in melanoma cells.[37] These observations imply a complex relationship between IL-6 and PD-L1. In this study, tumor-cell-intrinsic PD-L1 function enhanced the Jak2/Stat3 pathway and IL-6 production in NSCLC. Taken together, these results point to a novel positive feedback loop between IL-6 and PD-L1.

The role of cell-intrinsic PD-L1 in Stat3 signaling has been controversial. PD-L1 inhibits Stat3 to overcome IFN-induced cytotoxicity and trigger the inflammasome pathway.[17 38] In this study, PD-L1 was found to bind to and inhibit the tyrosine phosphatase PTP1B, a major negative regulator of Jak/Stat3 signaling,[28 39] subsequently activating Jak2/Stat3 signaling in NSCLC. In previous reports, PD-L1 formed a complex with p-Stat3, which was then translocated to the nucleus in response to hypoxia and facilitated the activity of p-Stat3 in the transcription of gasdermin C and the transcription factor early growth response 1 (EGR1).[11 16] In this study, nuclear PD-L1 was found to bind to p-Stat3 and enhance the transcription activity of p-Stat3 for IL-6 and other cytokines and chemokines in PD-L1-high NSCLC. Considering the functional role of nuclear PD-L1 in the transcription of molecules that recruit and activate MDSCs, strategies to impede nuclear translocation of PD-L1, such as HDAC inhibitors,[7 11] may improve the efficacy of ICI therapy in PD-L1-high NSCLC.

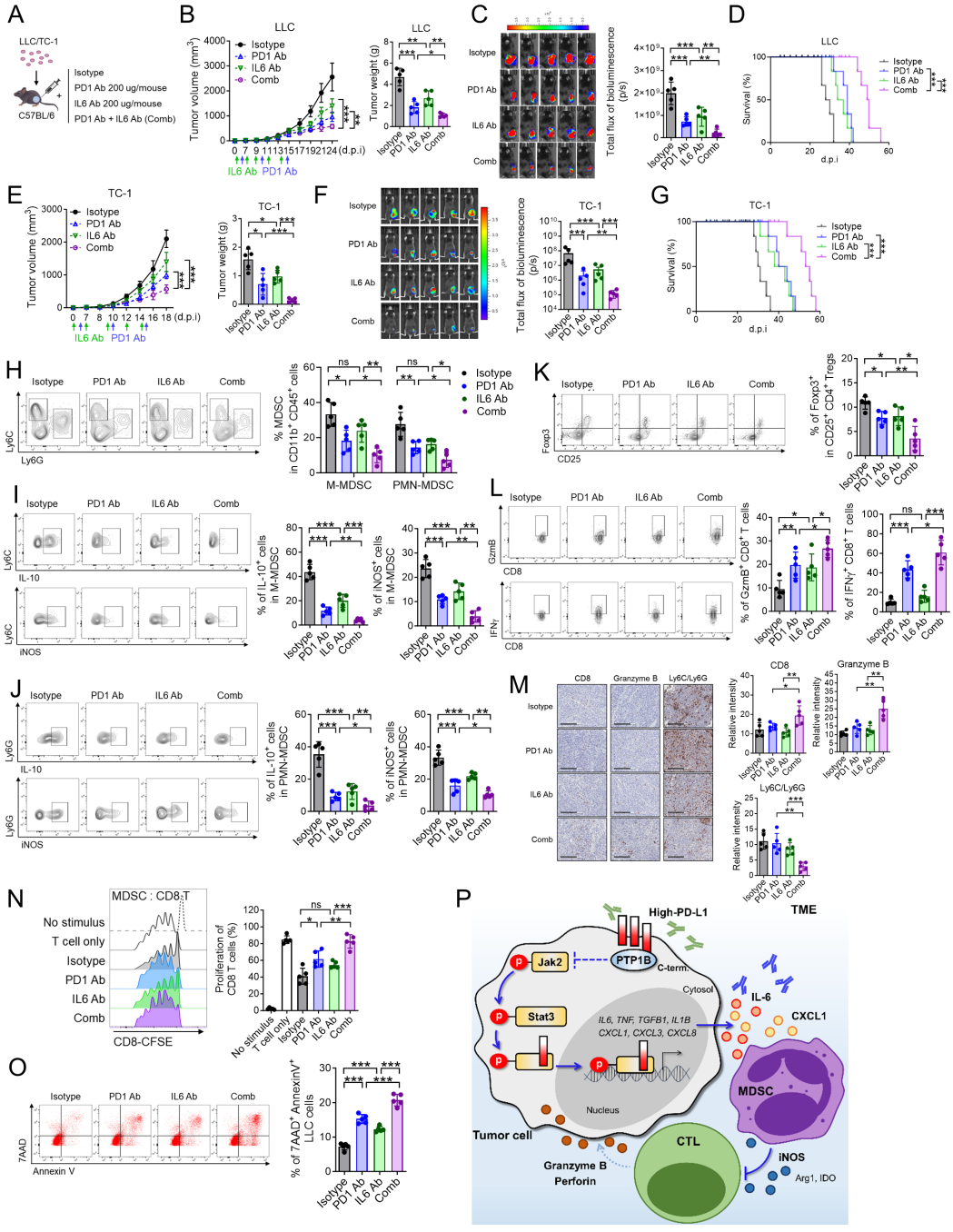

Figure 7 Combined blockade of IL-6 and PD-1 efficiently controls tumor growth and elicits antitumor immune response. (A) Wild-type LLC or TC-1 cells were injected subcutaneously into the flanks of C57BL/6 mice. For anti-PD-1 immunotherapy, the mice were injected intraperitoneally with 200 µg of anti-PD-1 antibody every 5 days a total of three times. For anti-IL-6 antibody (Ab) treatment, the mice were injected intraperitoneally with 200 µg of anti-mouse IL-6 Ab every 3 days for a total of five times. (B, C, E, F) Tumor size was measured every 2–3 days using calipers. Tumor volume was measured using the IVIS Spectrum imaging system, after which the mice were euthanized and tumor weight was determined. (D, G) Mice were observed for survival every 2–3 days. Differences in survival were compared using a log-rank test. (H–L) The immune cell populations of LLC tumors were assessed using flow cytometry. (M) IHC staining of $CD8^+$, $GzmB^+$, and $Ly6C/Ly6G^+$ cells in LLC tumors (scale bar=200 µm). (N) MDSCs isolated from LLC tumors were cultured with CFSE-labeled anti-CD3/CD28 bead-stimulated $CD8^+$ T-cells isolated from tumor-free C57BL/6 mice; the proliferation of $CD8^+$ T-cells was then assessed using flow cytometry. (O) $CD8^+$ T-cells isolated from LLC tumors were cultured with CFSE-labeled wild-type LLC cells for 24 hours. The cells were then stained with 7-AAD and Annexin V, and LLC viability was determined by flow cytometry. (P) Schematic diagram showing that tumor-cell-intrinsic PD-L1 activates Jak2/Stat3 signaling and contributes to IL-6 production, which drives MDSC-mediated immunosuppression in PD-L1-high lung cancer. Combined therapy targeting PD-1 and IL-6 may thus be effective in tumor control by restoring antitumor immunity. The data are presented as the mean±SEM of five independent experiments. *p<0.05, **p<0.01, ***p<0.001. CFSE, carboxyfluorescein succinimidyl ester; LLC, Lewis lung carcinoma; MDSC, myeloid-derived suppressor cell.

A recent transcriptomic analysis revealed that IL-6/Jak/Stat3 pathway enrichment in tumor tissues was associated with a favorable response to ICIs in patients with NSCLC.[40] However, in other studies, increased IL-6 levels in the plasma or tissues of patients with NSCLC predicted unfavorable outcomes after ICI therapy.[36 41 42] Notably, in our study, while the IL-6/Jak/Stat3 pathway was enriched in tumors from ICI responders with PD-L1-low NSCLC, it was enriched in ICI non-responders with PD-L1-high NSCLC. Additionally, in our ICI cohorts, high IL-6 expression was associated with poor clinical outcomes after ICI therapy in patients with PD-L1-high NSCLC but not in those with PD-L1-low NSCLC. These findings imply a complex role for IL-6 as a biomarker for ICI responsiveness, depending on PD-L1 status. Nonetheless, it may predict a poor response and outcome after ICI therapy, particularly in patients with PD-L1-high NSCLC.

Notably, a study that used a dataset from our ICI-RNA-seq cohort and the cell-deconvolution method for a type-specific transcriptome revealed that the tumor cells of non-responders had higher IL-6 expression, whereas the tumor-infiltrating T-cells of responders had higher IL-6 levels.[42] The enriched IL-6/Jak/Stat3 pathway observed in ICI responders with PD-L1-low NSCLC in this study may, therefore, have been derived from immune cells, but this needs to be validated by additional studies.

In this study, combined therapy targeting IL-6 and the PD-1/PD-L1 pathway effectively controlled tumors by mitigating MDSC-mediated immunosuppression in a mouse lung tumor model. IL-6 blockade, when combined with ICI therapy, efficiently controlled tumor growth and promoted antitumor immunity in preclinical cancer models.[36 43] Furthermore, IL-6 blockade suppressed ICI-induced autoimmune toxicity but potentiated antitumor immunity.[43 44] Based on these findings, phase 2 clinical trials combining IL-6 blockade with ICIs have been conducted in patients with melanoma and NSCLC (NCT03999749, NCT04940299, and NCT04691817). However, IL-6 blockade exacerbated tumor growth in a RET-transgenic mouse melanoma model.[23] Recently, JAK inhibitors were shown to enhance the efficacy of anti-PD-1 immunotherapy by modulating myeloid cells and T-cells in early-phase clinical trials for patients with Hodgkin lymphoma and NSCLC.[45 46] These findings underscore the need for further research of the IL-6/Jak/Stat3 pathway before it can be fully harnessed for cancer immunotherapy.

PD-L1 is also expressed on T-cells and, when engaged, promotes immune tolerance and tumor progression.[47 48] A recent study showed that T-cell-intrinsic intracellular PD-L1 suppressed the effector function of CD8 T-cells and antitumor immunity, effects that were reversed by T-cell-intrinsic PD-L1 knockdown.[49] Given that the intrinsic function of PD-L1 in both tumor cells and T-cells drives immunosuppression in cancer, targeting PD-L1 using antibodies or agents that degrade or relocate PD-L1 presents an intriguing avenue for future cancer therapy.[4 5 12]

This study has several limitations. First, we did not specifically examine the role of the PD-L1/Jak/Stat3/IL-6 pathway in M-MDSCs and PMN-MDSCs, particularly in the context of in vitro experiments. Second, we used conventional phenotypic markers to isolate MDSCs from PBMCs without conducting functional studies to characterize these cells further. Despite Ficoll gradient separation, $CD15^+$ low-density neutrophils would be included in the "human MDSC cells" used for co-culture experiments. Third, the cells isolated from the spleens of tumor-free (naïve) mice using FACS for in vivo experiments would be $CD11b^+Ly6G^+$ and $CD11b^+Ly6C^+$ myeloid cells rather than bona fide MDSCs. Fourth, we performed all in vivo tumor studies using the syngeneic LLC model. Use of a transgenic autochthonous in vivo model of NSCLC such as the $p53^{-/-}Kras^{G12D}$ mouse would be an excellent choice to improve the robustness of our findings.

CONCLUSIONS

In summary, our study demonstrated that the tumor-cell-intrinsic functions of PD-L1 activate the IL-6/Jak/Stat3 pathway, which in turn drives immunosuppression by MDSCs. This cell-intrinsic PD-L1/IL-6/MDSC axis may serve as both a potential biomarker for ICI therapy and a target for improving the efficacy of ICIs in patients with PD-L1-high NSCLC.

Author affiliations
[1]Cancer Research Institute, Seoul National University, Seoul, Korea (the Republic of)
[2]Interdisciplinary Program of Cancer Biology, Seoul National University Graduate School, Seoul, Korea (the Republic of)
[3]Department of Pathology, Seoul National University Hospital, Seoul National University College of Medicine, Seoul, Korea (the Republic of)
[4]Department of Pathology, Korea University Guro Hospital, Korea University College of Medicine, Seoul, Korea (the Republic of)
[5]Department of Pathology, Boramae Medical Center, Seoul National University, Seoul, Korea (the Republic of)
[6]Department of Biomedical Sciences, Seoul National University College of Medicine, Seoul, Korea (the Republic of)
[7]BK21 FOUR Biomedical Science Project, Seoul National University College of Medicine, Seoul, Korea (the Republic of)
[8]Department of Pharmacology, Seoul National University College of Medicine, Seoul, Korea (the Republic of)
[9]Seoul National University College of Medicine, Seoul, Korea (the Republic of)
[10]Institute of Allergy and Clinical Immunology, Seoul National University Medical Research Center, Seoul, Korea (the Republic of)
[11]Department of Internal Medicine, Seoul National University Hospital, Seoul National University College of Medicine, Seoul, Korea (the Republic of)
[12]Division of Hematology-Oncology, Department of Medicine, Samsung Medical Center, Gangnam-gu, Korea (the Republic of)
[13]Department of Health Sciences and Technology, Samsung Advanced Institute of Health Sciences and Technology, Sungkyunkwan University, Seoul, Korea (the Republic of)
[14]BK21 FOUR Smart Healthcare, Seoul National University College of Medicine, Seoul, Korea (the Republic of)

Acknowledgments Professor Seung Hyeok Seok at the Department of Microbiology and Immunology, Seoul National University, Seoul, Republic of Korea, kindly provides the LLC cells with a luciferase reporter.

Contributors YKJ and HJ conceptualized and designed the study. HJ, KJ, SK, HaK, YL, SHL, YKC, HoK, BK, and S-HL. acquired the data. HJ, KJ, SK, SGS, C-HL, BK, DHC and YKJ interpreted and analyzed the data. C-HL, HYK, BK, S-HL and DHC provided

resources and methodology. HJ, KJ, SK, SGS and YKJ drafted the manuscript and figures. All authors revised edited, and approved the final version of the manuscript. YKJ is responsible for the overall content (as guarantor).

Funding This work was supported by the Basic Research Program through the National Research Foundation of Korea (NRF) (Grant Nos. 2020R1A4A1017515, RS-2023-00217571, RS-2023-00252806), funded by the Ministry of Science and ICT; the Seoul National University Cancer Research Institute Research Program (Grant No. 0431-20220017), funded by the Seoul National University; a grant funded by the Korean Association for Lung Cancer (KALC-202312); by the Health Fellowship Foundation (2024, to HJ); a NRF grant funded by the Ministry of Science and ICT (Grant Nos. 2020R1F1A1070825, 2020R1A2C3006535) and the Post-Genome Technology Development Program (Business Model Development Driven by Clinico-Genomic Database for Precision Immuno-oncology) funded by the Ministry of Trade, Industry and Energy (MOTIE) (Grant No. 10067758), Republic of Korea.

Competing interests None declared.

Patient consent for publication Not applicable.

Ethics approval The IRBs of Seoul National University Hospital (SNUH) (no. H-1905-115-1035) and Samsung Medical Center (nos. SMC-2013-10-112 and SMC-2018-03-130) approved the study protocol of ICI-RNA-seq cohort. The IRB of SNUH approved the study protocols of the ICI-serum and ICI-IHC cohort (nos. 2310-090-1476 and 1408-007-598). Analysis of resected patient lung cancer tissues was performed according to the protocol approved by the IRB of SNUH (no. 1408-007-598). Human PBMCs were isolated from healthy donors and analyzed according to the protocol approved by the IRB of SNUH (no. 2203-174-1311). All participants provided written informed consent. All mice experiments were conducted under the conditions with the animal care guidelines approved by the Institutional Animal Care and Use Committee (IACUC) of SNU (no. SNU-220303-5) and SNUH (no. 22-0082-S1A0(1)), and by the Institutional Biosafety Committee of SNU (no. SNUIBC-P231016-1).

Provenance and peer review Not commissioned; externally peer reviewed.

Data availability statement Data are available in a public, open access repository. Data are available on reasonable request. RNA-seq data sets for ICI cohort are available in the Gene Expression Omnibus database (accession number GSE285029). Other data generated in this study are available in the article and its supplementary data files or on request from the corresponding author.

ORCID iDs
Bhumsuk Keam http://orcid.org/0000-0002-2974-675X
Yoon Kyung Jeon http://orcid.org/0000-0001-8466-9681

REFERENCES

1 Doroshow DB, Bhalla S, Beasley MB, *et al*. PD-L1 as a biomarker of response to immune-checkpoint inhibitors. *Nat Rev Clin Oncol* 2021;18:345–62.
2 Man J, Millican J, Mulvey A, *et al*. Response Rate and Survival at Key Timepoints With PD-1 Blockade vs Chemotherapy in PD-L1 Subgroups: Meta-Analysis of Metastatic NSCLC Trials. *JNCI Cancer Spectr* 2021;5:pkab012.
3 Pardoll DM. The blockade of immune checkpoints in cancer immunotherapy. *Nat Rev Cancer* 2012;12:252–64.
4 Kornepati AVR, Vadlamudi RK, Curiel TJ. Programmed death ligand 1 signals in cancer cells. *Nat Rev Cancer* 2022;22:174–89.
5 Yamaguchi H, Hsu JM, Yang WH, *et al*. Mechanisms regulating PD-L1 expression in cancers and associated opportunities for novel small-molecule therapeutics. *Nat Rev Clin Oncol* 2022;19:287–305.
6 Escors D, Gato-Cañas M, Zuazo M, *et al*. The intracellular signalosome of PD-L1 in cancer cells. *Signal Transduct Target Ther* 2018;3:26.
7 Gao Y, Nihira NT, Bu X, *et al*. Acetylation-dependent regulation of PD-L1 nuclear translocation dictates the efficacy of anti-PD-1 immunotherapy. *Nat Cell Biol* 2020;22:1064–75.
8 Du W, Zhu J, Zeng Y, *et al*. KPNB1-mediated nuclear translocation of PD-L1 promotes non-small cell lung cancer cell proliferation via the Gas6/MerTK signaling pathway. *Cell Death Differ* 2021;28:1284–300.
9 Cheon H, Holvey-Bates EG, McGrail DJ, *et al*. PD-L1 sustains chronic, cancer cell-intrinsic responses to type I interferon, enhancing resistance to DNA damage. *Proc Natl Acad Sci U S A* 2021;118:e2112258118.
10 Kornepati AVR, Boyd JT, Murray CE, *et al*. Tumor Intrinsic PD-L1 Promotes DNA Repair in Distinct Cancers and Suppresses PARP Inhibitor-Induced Synthetic Lethality. *Cancer Res* 2022;82:2156–70.
11 Yu J, Zhuang A, Gu X, *et al*. Nuclear PD-L1 promotes EGR1-mediated angiogenesis and accelerates tumorigenesis. *Cell Discov* 2023;9:33.
12 Tu X, Qin B, Zhang Y, *et al*. PD-L1 (B7-H1) Competes with the RNA Exosome to Regulate the DNA Damage Response and Can Be Targeted to Sensitize to Radiation or Chemotherapy. *Mol Cell* 2019;74:1215–26.
13 Chang C-H, Qiu J, O'Sullivan D, *et al*. Metabolic Competition in the Tumor Microenvironment Is a Driver of Cancer Progression. *Cell* 2015;162:1229–41.
14 Jeong H, Koh J, Kim S, *et al*. Epithelial-mesenchymal transition induced by tumor cell-intrinsic PD-L1 signaling predicts a poor response to immune checkpoint inhibitors in PD-L1-high lung cancer. *Br J Cancer* 2024;131:23–36.
15 Kim S, Jang J-Y, Koh J, *et al*. Programmed cell death ligand-1-mediated enhancement of hexokinase 2 expression is inversely related to T-cell effector gene expression in non-small-cell lung cancer. *J Exp Clin Cancer Res* 2019;38:462.
16 Hou J, Zhao R, Xia W, *et al*. PD-L1-mediated gasdermin C expression switches apoptosis to pyroptosis in cancer cells and facilitates tumour necrosis. *Nat Cell Biol* 2020;22:1264–75.
17 Theivanthiran B, Evans KS, DeVito NC, *et al*. A tumor-intrinsic PD-L1/NLRP3 inflammasome signaling pathway drives resistance to anti-PD-1 immunotherapy. *J Clin Invest* 2020;130:133055:2570–86:.
18 Jones SA, Jenkins BJ. Recent insights into targeting the IL-6 cytokine family in inflammatory diseases and cancer. *Nat Rev Immunol* 2018;18:773–89.
19 Fisher DT, Appenheimer MM, Evans SS. The two faces of IL-6 in the tumor microenvironment. *Semin Immunol* 2014;26:38–47.
20 Weber R, Groth C, Lasser S, *et al*. IL-6 as a major regulator of MDSC activity and possible target for cancer immunotherapy. *Cell Immunol* 2021;359:104254.
21 Tsukamoto H, Fujieda K, Senju S, *et al*. Immune-suppressive effects of interleukin-6 on T-cell-mediated anti-tumor immunity. *Cancer Sci* 2018;109:523–30.
22 Caetano MS, Zhang H, Cumpian AM, *et al*. IL6 Blockade Reprograms the Lung Tumor Microenvironment to Limit the Development and Progression of K-ras-Mutant Lung Cancer. *Cancer Res* 2016;76:3189–99.
23 Weber R, Riester Z, Hüser L, *et al*. IL-6 regulates CCR5 expression and immunosuppressive capacity of MDSC in murine melanoma. *J Immunother Cancer* 2020;8:e000949.
24 Neo SY, Tong L, Chong J, *et al*. Tumor-associated NK cells drive MDSC-mediated tumor immune tolerance through the IL-6/STAT3 axis. *Sci Transl Med* 2024;16:eadi2952.
25 Fisher DT, Chen Q, Skitzki JJ, *et al*. IL-6 trans-signaling licenses mouse and human tumor microvascular gateways for trafficking of cytotoxic T cells. *J Clin Invest* 2011;121:3846–59.
26 Liberzon A, Birger C, Thorvaldsdóttir H, *et al*. The Molecular Signatures Database (MSigDB) hallmark gene set collection. *Cell Syst* 2015;1:417–25.
27 Chen C, Li S, Xue J, *et al*. PD-L1 tumor-intrinsic signaling and its therapeutic implication in triple-negative breast cancer. *JCI Insight* 2021;6:e131458.
28 Morris R, Keating N, Tan C, *et al*. Structure guided studies of the interaction between PTP1B and JAK. *Commun Biol* 2023;6:641.
29 Lasser SA, Ozbay Kurt FG, Arkhypov I, *et al*. Myeloid-derived suppressor cells in cancer and cancer therapy. *Nat Rev Clin Oncol* 2024;21:147–64.
30 Limagne E, Richard C, Thibaudin M, *et al*. Tim-3/galectin-9 pathway and mMDSC control primary and secondary resistances

to PD-1 blockade in lung cancer patients. *Oncoimmunology* 2019;8:e1564505.
31 He Z-N, Zhang C-Y, Zhao Y-W, *et al*. Regulation of T cells by myeloid-derived suppressor cells: emerging immunosuppressor in lung cancer. *Discov Oncol* 2023;14:185.
32 Liang M, Sun Z, Chen X, *et al*. E3 ligase TRIM28 promotes anti-PD-1 resistance in non-small cell lung cancer by enhancing the recruitment of myeloid-derived suppressor cells. *J Exp Clin Cancer Res* 2023;42:275.
33 Lee JW, Zhang Y, Eoh KJ, *et al*. The Combination of MEK Inhibitor With Immunomodulatory Antibodies Targeting Programmed Death 1 and Programmed Death Ligand 1 Results in Prolonged Survival in Kras/p53-Driven Lung Cancer. *J Thorac Oncol* 2019;14:1046–60.
34 Orillion A, Hashimoto A, Damayanti N, *et al*. Entinostat Neutralizes Myeloid-Derived Suppressor Cells and Enhances the Antitumor Effect of PD-1 Inhibition in Murine Models of Lung and Renal Cell Carcinoma. *Clin Cancer Res* 2017;23:5187–201.
35 Chan L-C, Li C-W, Xia W, *et al*. IL-6/JAK1 pathway drives PD-L1 Y112 phosphorylation to promote cancer immune evasion. *J Clin Invest* 2019;129:3324–38.
36 Liu C, Yang L, Xu H, *et al*. Systematic analysis of IL-6 as a predictive biomarker and desensitizer of immunotherapy responses in patients with non-small cell lung cancer. *BMC Med* 2022;20:187.
37 Tsukamoto H, Fujieda K, Miyashita A, *et al*. Combined Blockade of IL6 and PD-1/PD-L1 Signaling Abrogates Mutual Regulation of Their Immunosuppressive Effects in the Tumor Microenvironment. *Cancer Res* 2018;78:5011–22.
38 Gato-Cañas M, Zuazo M, Arasanz H, *et al*. PDL1 Signals through Conserved Sequence Motifs to Overcome Interferon-Mediated Cytotoxicity. *Cell Rep* 2017;20:1818–29.
39 Feldhammer M, Uetani N, Miranda-Saavedra D, *et al*. PTP1B: a simple enzyme for a complex world. *Crit Rev Biochem Mol Biol* 2013;48:430–45.
40 Ravi A, Hellmann MD, Arniella MB, *et al*. Genomic and transcriptomic analysis of checkpoint blockade response in advanced non-small cell lung cancer. *Nat Genet* 2023;55:807–19.
41 Keegan A, Ricciuti B, Garden P, *et al*. Plasma IL-6 changes correlate to PD-1 inhibitor responses in NSCLC. *J Immunother Cancer* 2020;8:e000678.
42 Naqash AR, McCallen JD, Mi E, *et al*. Increased interleukin-6/C-reactive protein levels are associated with the upregulation of the adenosine pathway and serve as potential markers of therapeutic resistance to immune checkpoint inhibitor-based therapies in non-small cell lung cancer. *J Immunother Cancer* 2023;11:e007310.
43 Hailemichael Y, Johnson DH, Abdel-Wahab N, *et al*. Interleukin-6 blockade abrogates immunotherapy toxicity and promotes tumor immunity. *Cancer Cell* 2022;40:509–23.
44 Holmstroem RB, Nielsen OH, Jacobsen S, *et al*. COLAR: open-label clinical study of IL-6 blockade with tocilizumab for the treatment of immune checkpoint inhibitor-induced colitis and arthritis. *J Immunother Cancer* 2022;10:e005111.
45 Zak J, Pratumchai I, Marro BS, *et al*. JAK inhibition enhances checkpoint blockade immunotherapy in patients with Hodgkin lymphoma. *Science* 2024;384:eade8520.
46 Mathew D, Marmarelis ME, Foley C, *et al*. Combined JAK inhibition and PD-1 immunotherapy for non-small cell lung cancer patients. *Science* 2024;384:eadf1329.
47 Diskin B, Adam S, Cassini MF, *et al*. PD-L1 engagement on T cells promotes self-tolerance and suppression of neighboring macrophages and effector T cells in cancer. *Nat Immunol* 2020;21:442–54.
48 Fanelli G, Romano M, Nova-Lamperti E, *et al*. PD-L1 signaling on human memory CD4+ T cells induces a regulatory phenotype. *PLoS Biol* 2021;19:e3001199.
49 Wang X, Lu L, Hong X, *et al*. Cell-intrinsic PD-L1 ablation sustains effector CD8+ T cell responses and promotes antitumor T cell therapy. *Cell Rep* 2024;43:113712.